1
2

Effect of supercritical carbonation on the strength and heavy metal retention of cement-solidified fly ash

3
4
5

Xiaoxiong Zha[a,*], Jiaqian Ning[a], Mohamed Saafi[b], Lijun Dong[a], Jean-Baptiste Mawulé Dassekpo[a], Jianqiao Ye[b,*]

6
7   [a] Department of Civil and Environmental Engineering, Shenzhen Graduate School,
8   Harbin Institute of Technology, 518055 China
9   [b] Department of Engineering, Lancaster University, Lancaster LA1 4YR, UK
10   * Corresponding author.

11   E-mail address j.ye2@lancaster.ac.uk (J. Ye) and zhaxx@hit.edu.cn (X.X. Zha)

12

Abstract

14   This paper presents both experimental and multi-physics studies on the carbonation and heavy

15   metal retention properties of cement-solidified fly ashes. Cement-solidified fly ash samples

16   with 40% and 60% fly ash ratios were tested for carbonation depth after being supercritically

17   carbonated. Tests were also carried out for compressive strength and retention capacity of heavy

18   metals of the samples before and after supercritical carbonation. Using CO_2 absorption instead

19   of calcium carbonate to measure carbonation degree, a multi-physics model was developed and

20   combined with a leaching model to study the impact of carbonation on Cu and Pb leaching from

21   the cement-solidified fly ash. The results show that supercritical carbonation has both positive

22   and negative impacts on the strength and retention capability of heavy metals of the cement-

23   solidified fly ashes, which suggests that both the carbonation conditions and the amount of fly

24   ash recycled in cementitious materials should be properly controlled to maximize potential

25   positive effect.

26

27
28   ***Keywords:*** Cement-solidified; supercritical carbonation; fly ash; compressive strength;

29   leaching rate.

1. Introduction

Protection of the public from hazardous pollutants in the environment has always been an important priority for most industrialized countries, where a significant portion of the pollutants is related to the increasing demands for energy. The data published by the International Energy Agency stated that the energy consumption had increased by 50.52% from 1990 to 2014. Consequently, the appearance of environmental problems poses a serious threat to the living environment of human beings, such as heavy metal pollution caused by municipal solid waste incineration (MSWI) fly ash [1, 2], global warming due to carbon dioxide (CO_2) emissions [3], and so forth.

Municipal solid waste (MSW) has been always one of the most challenging problems in the management of modern cities. There are about 254 million tons of garbage produced annually in China, namely approximately one kilogram per person per day, the total amount of which is about one third of the world's annual trash output [4]. The rapid growth of waste causes serious limitations in the development of a city, if it is not handled properly [5]**Error! Reference source not found.**. In recent years, MSWI has been widely used owing to its advantage on capacity reduction and energy recovery efficiency [6, 7]. However, the by-product of MSWI, such as fly ash [8], contains heavy metals that still have serious negative impact on the surrounding environment [9], or can even cause irreparable damage to human health. Therefore, the environmental threat from fly ash cannot be ignored and the development of an economic, efficient and eco-friendly application of fly ash is one of the most important measures to address the current situation.

From the perspective of the construction industry, fly ash can be used as a cement replacement material [10] to develop high performance concrete. Besides the superiority in the value of recycling [11] and CO_2 emissions [12], fly ash can also reduce hydration heat and improve workability [13], as well as durability of concrete [14]. A concrete component with a high fly ash replacement ratio has little impact on the bond strength with conventional concrete [15],

59 which may also have higher shear strength [16]. Hence, using MSWI fly ash as partial

60 replacement for cement in concrete mixes is potentially feasible [17].

61
62 To further develop the potential material, the mechanical properties, durability and leaching

63 performance of the cement-solidified fly ash were studied [18, 19]. Cement solidification

64 technology is an effective waste solidification method, which obviously reduces the leaching

65 toxicity of harmful substances, especially heavy metals, in cement-solidified fly ash [17].

66 Leaching tests were also conducted to verify the feasibility of the technology [14]. Leaching in

67 a solidified body varies with water-cement ratios and also types of leachants, e.g. deionized or

68 mineralized water. Pure water appeared more aggressive than mineralized water [20]. Moreover,

69 a multi-physics leaching model of a solidified body was also developed and the simulation

70 results were compared with those from leaching experiment of Sr and Cs [21].

71
72 Cement-based materials are porous, in which the pores form the channels that leak heavy metals,

73 resulting in a reduced capacity of retaining them in the solidified body [22]. Carbonation of

74 cement-based materials can improve the pore structure of the material, and therefore reduces

75 its porosity [23]. The technique has been used to treat waste to reduce leaching toxicity of

76 certain metals [24]. Recently, research on accelerated and supercritical carbonation, i.e.,

77 carbonation under elevated temperature and pressure were carried out [21]. When the

78 temperature and pressure of CO_2 exceed their respective critical states (T_c=31.26ºC,

79 P_c=7.39MPa), the CO_2 is said under its supercritical state (SCC) [25]. Other supercritical

80 carbonation models of cement mortar and cement include Refs. [13, 26, 27]. To study the effect

81 of carbonation on the leaching resistance of hazardous waste cement solidification, Zha et al.

82 [21] develop a model using the finite element software COMSOL Multiphysics. The parametric

83 studies from the numerical simulations revealed that carbonation could significantly improve

84 the retention capability of cementitious solids containing hazardous wastes.

85
86 In this paper, further modifications on, e.g, the carbonation rate equation, specific heat of CO_2

87 and change of porosity caused by carbonation, are made based on the simulation model

88 proposed by Zha et al. [27] for cement-solidified fly ash. The simplified form of the leaching

89 model [21] is adopted to estimate the leaching of Cu and Pb. The carbonation and leaching

90 models are used together to build a combined model for the multi-physics carbonation-leaching

91 problem. Then, carbonation, strength and leaching experiments are carried out for 40% and 60%

92 cement-solidified fly ash to validate the modified models and study the effect of carbonation

93 and fly ash ratio on the performance of the cement-solidified fly ash.

94
95 ## 2. Mathematical modeling

96 ### 2.1 Equations of supercritical carbonation process

97 Based on the natural carbonation model by Saetta et al. [23], Zha et al. [27] proposed a model

98 for supercritical carbonation, where (1) Darcy's law was used in place of Fick's law; and (2)

99 the change of CO_2 concentration in pore solution was assumed to be equal to that of its solubility,

100 i.e., assuming that there was always sufficient dissolved CO_2 to participate in the carbonation

101 reaction under supercritical carbonation conditions.

102
103 The equations to be solved include the carbonation rate equation, the mass conservation

104 equation of CO_2, the gas-liquid two-phase flow equations and the energy conservation equation,

105 as shown in equation (1).

$$
\begin{cases}
\dfrac{\partial R_c}{\partial t} = \alpha_1 f_1(h) f_2(g) f_3(R_c) f_4(T) \\[2mm]
\dfrac{\partial g}{\partial t} = \dfrac{\partial m_c}{\partial t} \\[2mm]
\dfrac{\partial (n S_\alpha \rho_\alpha)}{\partial t} + \nabla \cdot (\rho_\alpha \overset{v}{\mu}_\alpha) = q_\alpha \\[2mm]
\overset{v}{\mu}_\alpha = -\dfrac{k \cdot k_{ra}}{\mu_\alpha}(\Delta P_\alpha) \\[2mm]
(\rho C_q)_{eff} \dfrac{\partial T}{\partial t} = \nabla \cdot (k_{eff} \nabla T) - (C_g \rho_g \overset{uuv}{\mu}_g + C_w \rho_w \overset{uuv}{\mu}_w) \cdot \nabla T
\end{cases}
\tag{1}
$$

106 where R_c is the degree of carbonation; α_1 is the carbonation rate coefficient, indicating the

107 variation rate of carbonation degree under ideal conditions; $f_1(h)$, $f_2(g)$, $f_3(R_c)$ and $f_4(T)$ denote,

108 respectively, the effect of humidity, CO_2 concentration, carbonation degree and temperature on

109 the carbonation rate; g is the mass concentration of CO_2; m_c is the solubility; n is the porosity

of the cement-based materials; S_α, ρ_α, $\overset{v}{\mu}_\alpha$, q_α, $k_{r\alpha}$, μ_α, P_α and C_α are the saturation, density, Darcy

velocity, source item accounting for chemical reaction or precipitation, relative permeability

coefficient, dynamic viscosity, pressure and specific heat of component α, respectively. The

subscript, α, can be either g or w denoting gas or liquid phases, respectively; k is the inherent

permeability; $(\rho C_q)_{eff}$ is the equivalent heat capacity; k_{eff} is the equivalent thermal conductivity.

2.2 Modification of carbonation equations

Numerous studies on supercritical carbonation of cement-based materials have been conducted

[27-29]. However, the adopted theory, e.g., equation (1), is not generally applicable to all the

cement-based materials, especially to the materials with admixtures. In this paper, some

modifications are introduced to extend its applicability to include cement-solidified fly ash.

2.2.1 Modified carbonation reaction rate equation

The main chemical reactions during the carbonation process of cement-based materials are

shown in equation (2), in which C-S-H stands for calcium silicate hydrate.

$$\begin{cases} Ca(OH)_2 + CO_2 \rightarrow CaCO_3 + H_2O \\ C\text{-}S\text{-}H + CO_2 \rightarrow CaCO_3 + SiO_2 \cdot nH_2O \end{cases} \tag{2}$$

The carbonation rate was estimated in the previous model [27] on the basis of the measurement

of the calcium carbonates generated during the process, i.e., the carbonation degree is calculated

by the following equation:

$$R_c = \frac{cc}{cc_{max}} \tag{3}$$

where cc is the amount of calcium carbonate produced in the carbonation process and cc_{max} is

the cc when the material is fully carbonated.

However, the using of calcium carbonate production to measure carbonation degree has its

limitations and can be inaccurate in assessing carbonation degree. Calcium carbonate generated

by carbonation is an insoluble substance which can be trace dissolved in the pore solution, and

reacts with CO_2 and water to form dissolvable calcium bicarbonate under high levels of

dissolved CO_2 [30]. Also, calcium carbonate exists not only with the form of the single-

compound in carbonated cement-based materials, but also binds to other remaining products, e.g. to SiO_2 and H_2O to form $xCaCO_3 \cdot ySiO_2 \cdot zH_2O$ [31]. This paper proposed an alternative estimation of carbonation degree based on measuring the CO_2 absorbed in the carbonation process, which takes a full account of all reactions with CO_2. Hence the following carbonation degree equation is proposed:

$$R_c = \frac{c}{c_{max}} \tag{4}$$

where c is the CO_2 absorbed by cement-based materials, c_{max} is the CO_2 absorbed after being fully carbonated, which can be assessed by phenolphthalein indicator [32] that changes the color of any non-carbonated cement to pink. The indicator is a 1% phenolphthalein ethanol solution with 1g phenolphthalein and 95% ethanol diluted to 100 ml. The calculation method of c_{max} will be discussed in the next section.

Introducing equation (4) into the first equation of equation (1) yields,

$$\frac{\partial c}{\partial t} = \alpha_1 f_1(h) f_2(g) f_3(c) f_4(T) \tag{5}$$

where $f_3(c)$ denotes the effect of the absorbed CO_2 on the carbonation rate, which is calculated by.

$$f_3(c) = c_{max} - c \tag{6}$$

2.2.2 Determination of cmax

The calculation of the maximum CO_2 absorbed per unit volume by cement-based materials in the ideal state is proposed below, which is related to the amount of calcium, iron, and aluminum oxides in the material [33].

$$c_{max} = m_0 \left(\frac{[CaO]}{M_{CaO}} - 4\frac{[Fe_2O_3]}{M_{Fe_2O_3}} - 4\frac{[Al_2O_3]}{M_{Al_2O_3}} \right) \tag{7}$$

where, m_0, in kg/m^3, is the amount of cement per cubic meter cement-based materials; M and [*], in which * can be CaO, Fe_2O_3 or Al_2O_3, represent the molar mass and the mole fraction of metallic oxide in cement, respectively. In equation (7), M_{CaO} = 0.056 kg/mol, M_{Fe2O3} = 0.16

155   kg/mol and $M_{Al2O3} = 0.102$ kg/mol.

156

157   Because the dimension of c_{max} is mol·m^{-3} in equation (7) and kg·m^{-3} in equation (6), Equation

158   (7) is modified as follows:

$$c_{\max} = M_c m_0 \left(\frac{[CaO]}{M_{CaO}} - 4\frac{[Fe_2O_3]}{M_{Fe_2O_3}} - 4\frac{[Al_2O_3]}{M_{Al_2O_3}} \right) \tag{8a}$$

159   where M_c is the molar mass of CO_2 ($M_c = 0.044$ kg/mol).

160

161   When cement is partially replaced with admixtures that have similar chemical components, (e.g.

162   fly ash with major chemical constituents CaO, SiO_2, Al_2O_3 and Fe_2O_3), the hydration and

163   carbonation of the resulting admixtures should be considered. However, the chemical

164   composition of fly ashes depends on the characteristics and composition of the coal burned in

165   e.g., a power station. Berry [22] demonstrated that there was a wide range of fly ash

166   compositions. Fly ash is generally classified as Low-calcium Fly Ash (LFA, <10% CaO) and

167   High-calcium Fly Ash (HFA, ≥10% CaO). For LFA, the c_{max} calculated by equation (8a) using

168   the fly ash compositions in Refs. [34, 35] is negative, and for HFA, the c_{max} calculated using the

169   fly ash compositions in Ref. [36] is ignorable when compared to that calculated for Ordinary

170   Portland Cement (OPC) [37]. Thus, in this paper, the contribution of fly ash to CO_2 absorption

171   of the cement-solidified is ignored.

172

173   Additionally, the amount of CO_2 absorbed during the carbonation process can be significantly

174   reduced due to the following two reasons: (1) cement-based materials are porous material

175   having large quantity of small and closed pores, which makes it difficult for the internal

176   materials to contact with CO_2; and (2) the precipitations generated in the carbonation process

177   accumulate on the inner surface of pores and clog the transport channels of CO_2, and then

178   prevent the reaction from proceeding. Thus, equation (8a) can be modified by introducing a

179   reduction factor, α, as shown in equation (8b) below.

$$c_{\max} = \alpha M_c m_0 \left(\frac{[CaO]}{M_{CaO}} - 4\frac{[Fe_2O_3]}{M_{Fe_2O_3}} - 4\frac{[Al_2O_3]}{M_{Al_2O_3}} \right) \tag{8b}$$

7

180

181 This paper combines numerical and experimental methods to estimate the reduction factor α,

182 as follows.

183 The CO_2 absorbed by a micro-volume of cement sample can be expressed as:

$$dm = R_c c_{max} dv \qquad (9)$$

184 where dm is the weight increment of dv after carbonation. Hence, m can be obtained by

185 integrating equation (9) over the whole cement sample.

$$m = \iiint_V R_c c_{max} dv = c_{max} \iiint_V R_c dv \qquad (10)$$

186 where m is the weight increase of cement sample after carbonation. The cylindrical Ordinary

187 Portland Cement (OPC) paste samples having the same diameter and height of 50mm were

188 used for carbonation. The chemical components of the OPC are CaO, Fe_2O_3 and Al_2O_3 with

189 weights of 61.87%, 5.26% and 5.14%, respectively [37]. The average weight increase measured

190 after carbonation was about 4.21g. A numerical model was developed and calibrated against

191 the experimental c_{max}, and $\iiint_V R_c dv$ was calculated by volume integration using COMSOL.

192 By combining the experiment and simulation results, the reduction factor calculated by

193 equations (10) and (8b) was α=0.178, which, in principal, is affected by multi-factors, such

194 as composition, mixing rule, pore characteristics, etc. Because of the limitation of the

195 experiments, 0.178 was used in the simulations (section 3) as the reduction factor for all the

196 CCFC composites and verified against the experimental results (section 4). Clearly, further

197 studies on the relationship between the reduction factor and the influential factors are needed,

198 which requires additional extensive experimental work.

199

200 ### 2.2.3 Modification on the CO_2 specific heat

201 The specific heat of CO_2 at constant pressure was adopted previously in the equation (1).

202 However, the pressure may change in a carbonation process, due to, e.g. a gradual reduction of

203 available CO_2 as carbonation is progressing. Naturally, the effect of pressure on the specific

204 heat of CO_2 should be considered. Researches on specific heat of CO_2 for different temperature

205 and pressure have been conducted by Li et al. [38] and Shi et al. [39]. The specific heat for 35°C

206 and a pressure of 7.0 to 8.0MPa, which was proposed by Shi et al. [39], is used here for the

207 supercritical condition, as follows:

$$C_c = \frac{40 + 11.5 \times (P_c - 7)}{M_c} \tag{11}$$

208 where P_c, M_c are the pressure and molar mass of CO_2, respectively.

2.2.4 Modification on the change of porosity

210 The change in porosity is the key factor for its close link to the leaching behavior of the

211 solidified cement. The following equation [40] was adopted previously in Zha et al. [27]:

$$n = \begin{cases} n_0(1 - 0.5R_c) & 0 \le R_c \le 0.4 \\ 0.8 \cdot n_0 & 0.4 \le R_c \le 1 \end{cases} \tag{12}$$

212 where n_0 is the porosity of the cement-based materials before carbonation.

213
214 Equation (12) only considers the effect of $Ca(OH)_2$ on porosity and ignores the effect of other

215 materials in the cement-based materials, such as C-S-H, un-hydrated $2CaO \cdot SiO_2$ and

216 $3CaO \cdot SiO_2$. Shen et al. [26] reported that the porosity of cement-based materials after

217 carbonation could be reduced by more than 50%, which was larger than the value calculated by

218 equation (12). Other literatures [21, 26, 41] also mentioned that porosity reduction could reach

219 up to above 70%. Hence, a mathematical model based on the experiment results of Zha et al.

220 [21], which is more accurate to reflect the variation of porosity during carbonation, is proposed

221 below:

$$n = \begin{cases} 0.4n_0 & 0.9 < R_c \le 1 \\ (0.85 - 0.5R_c)n_0 & 0.5 \le R_c \le 0.9 \\ (1 - 0.8R_c)n_0 & 0 \le R_c < 0.5 \end{cases} \tag{13}$$

2.3 Equation of leaching process

223 Zha et al. [21] established the partial differential equations of leaching process on the base of

224 Song et al. [42], which was according to the theory of non-equilibrium thermodynamic.

225 However, from GB/T 7023-2011 [43] for leaching tests, temperature is required to be constant

226 during the leaching process. The effect of temperature on the leaching is, therefore, neglected

9

227 in this paper, resulting in the following equation:

$$\nabla \cdot [\rho D \nabla C] - \lambda' \rho C + F = \rho \frac{\partial C}{\partial t} \tag{14}$$

228 where ρ is the density of the cement-based materials; D is the effective coefficient of diffusion;

229 λ' is the decay constant; F denotes the constant of absorption rate; C is the mass concentration

230 of the leaching elements, which varies with position and time, i.e., $C = f(x,y,z,t)$.

231 **2.4 Calculation of chemical activity factor**

232 The chemical activity factor was introduced to consider the effect of chemical fixation on the

233 diffusion coefficient in Zha et al. [21], and it was expressed by the ratio of free element

234 concentration to the total element. The respective values adopted for Sr and Cs was 0.7 and

235 0.06 [21]. Obviously, there is great difference in chemical activity factor for different elements,

236 which might depend on the pH and the chemical compositions in a cement-solidified material.

237
238 However, to the authors' best knowledge, there is no published researches on the calculation of

239 chemical activity factor during a carbonation process. In this paper, the chemical activity factors

240 of Pb and Cu were evaluated backwardly from the leaching experiment results against

241 carbonation degree. The obtained chemical activity factors of Pb and Cu are, respectively,

$$r_1 = (1 - 0.8 R_c^2) \cdot r_{01} \tag{15}$$

$$r_2 = (1 + 33 R_c) \cdot r_{02} \tag{16}$$

242 where r_1, r_2 are the chemical activity factors of Pb and Cu respectively during carbonation,

243 while r_{01} and r_{02} are their initial values.

244
245 **3. Numerical simulation**

246 **3.1 Geometric model**

247 In this section, carbonation and leaching of cement-solidified fly ash are simulated using the

248 finite element software COMSOL. The solidified cement block is cylindrical having the same

249 diameter and height of 50mm, which is placed within a cylindrical container of 120mm in
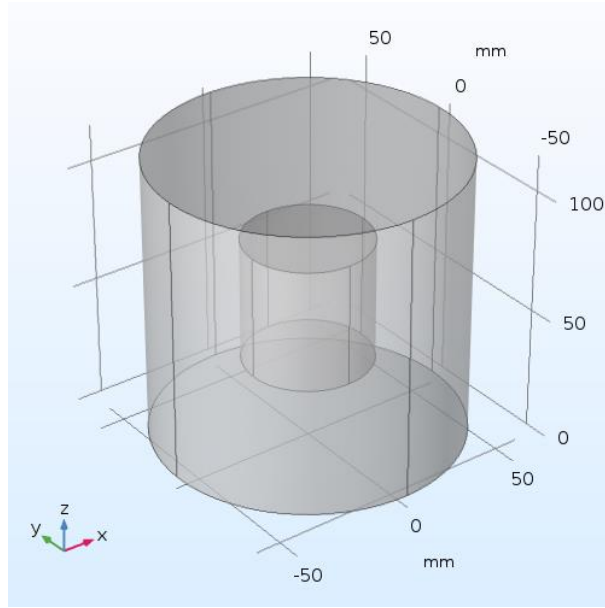
250 diameter and 115mm in height, as shown in Fig. 1.

Fig. 1 Geometry of carbonation and leaching model

3.2 Carbonation model

The carbonation process using the modified model in Section 2.2 is simulated by COMSOL with specified initial values of $R_c=0$, $P_g=1 atm$, $P_w=P_{w0}$, $T=T_0$ and $g=0$. Furthermore, the boundary conditions are modeled to represent, as close as possible, the actual reaction conditions in the laboratory experiments. As to the carbonation degree R_c and the CO_2 concentration g, both mathematically satisfied the Neumann boundary conditions, i.e., $\overset{\vee}{n} \cdot \nabla R_c = 0$, and $\overset{\vee}{n} \cdot \nabla g = 0$, respectively. The pressure and temperature used in the carbonation model were obtained from those measured in the experiments

The carbonation process is closely related to the chemical compositions in the cement-based materials. c_{max} was introduced previously in the paper to distinguish the content of CO_2 absorbed by different cement-based materials after full carbonation, and the cement-solidified samples with 40% and 60% fly ash were chosen to validate the modified model. The respective c_{max} calculated from equation (8b) are 46.6 kg/m³ and 34.1 kg/m³. After carbonated for 3 hours, the carbonation degree (R_c) obtained by Zha et al. [27] and the current model on the vertical sections across the center are shown in Fig. 2 and Fig. 3, respectively.
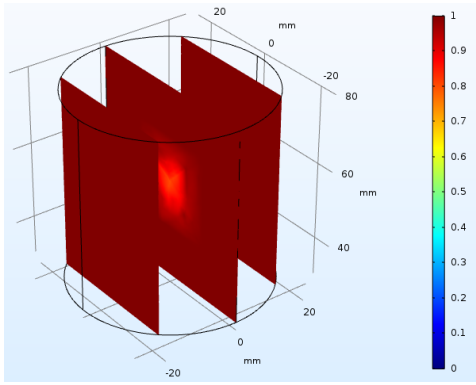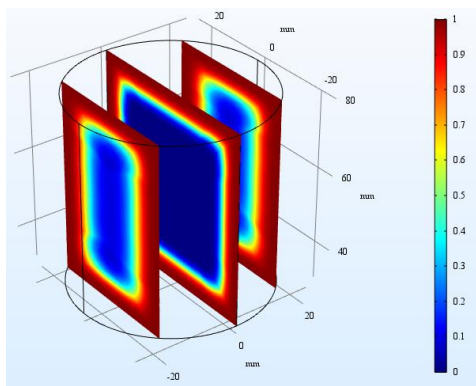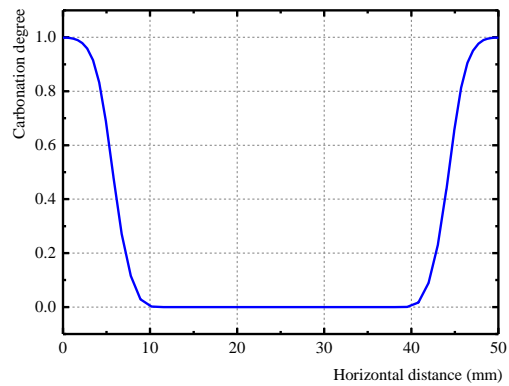
(a) R_c on sections-(40%, 60%)
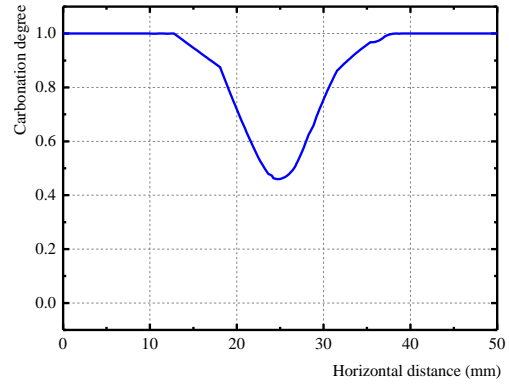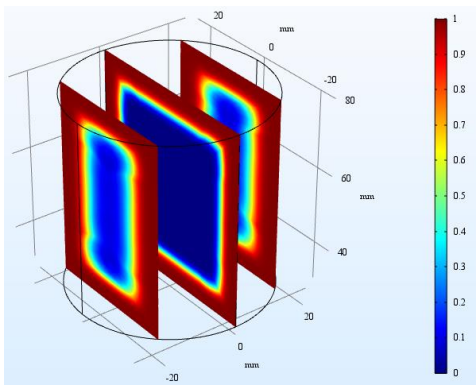
(b) R_c on transversal-(40%, 60%)

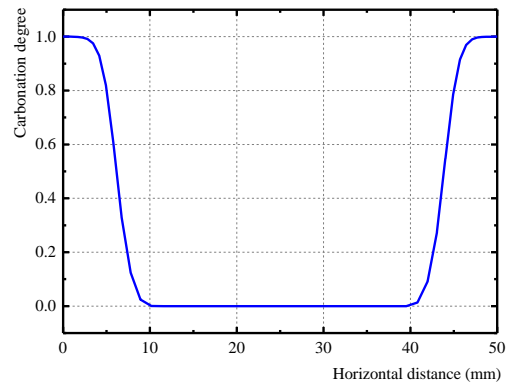Fig. 2 Simulation results based on Zha et al. [27]

(a) R_c on sections-(40%)

(b) R_c on transversal-(40%)

(c) R_c on sections-(60%)

(d) R_c on transversal-(60%)

Fig. 3 Simulation results based on the modified model

269
270 By using the model proposed in Zha et al. [27], it is not possible to consider the variation of fly

271 ash ratio in the calculation of carbonation degree, as shown in Fig. 2, while it can be taken into

272 account now by the modified model, as shown in Fig. 3. This is due to the introduction of c_{max}

273 that is different for different fly ash ratios (equation (8b)). In the simulation, a region is judged

12

as fully carbonated when its R_c is larger than 0.99. The carbonation depth from Fig. 2 is about 12mm, and those obtained from Fig. 3 are about 2.3mm and 3.5mm, respectively, for cement-solidified units with 40% and 60% fly ash. The experiment studies of these will be shown in Section 4.2.

3.3 Leaching model

In the leaching process, the initial ion concentration C in the leachant and the cement-solidified samples are set as $C=0$, $C=C_0$, respectively. The leaching from the samples to the leachant are assumed to be diffusion and due to concentration difference. The boundary of the leaching container is set as an insulation boundary, which is expressed by the Neumann boundary condition, $\vec{n} \cdot \nabla C = 0$.

3.4 Combined model

The independent carbonation and leaching models developed from the above sections are combined to form a continuous modeling process by introducing the carbonation results, e.g. the reduced porosity caused by carbonation, directly into the leaching model. It is worth noting that the diffusion coefficient of the leaching process should be set to zero at the carbonation process to prevent any leaching, while the carbonation rate coefficient is set to zero during the leaching process.

4. Experiments

4.1 Sample preparation

The main materials used in this study are Ordinary Portland Cement (OPC) and Fly Ash (FA). The fly ash was supplied from Nanshan waste incineration power plant in Shenzhen. To avoid the extreme situations, i.e. the strength of the sample is too low [44, 45] or the leaching concentration of heavy metals is too small to measure, 40% and 60% fly ash ratios in cement-solidified were investigated in this study. The mixture design of the samples is presented in Table 1. Each of the samples was cast into a cylinder having the same diameter and height of 50mm.

302   Table 1 The mixture of the cement-solidified fly ash samples

Mass ratio of fly ash	Components	Mass (g)	Mixing time(min)	Sample No.
40%	Cement	1500	15	2/3-1～2/3-19
	Fly ash	1000		
	Water	1400		
60%	Cement	1000	15	3/2-1～3/2-19
	Fly ash	1500		
	Water	1400		

303
304   The average initial Cu and Pb contents of the cement-solidified fly ash samples are shown in

305   Table 2, which were used also in the simulations (Section 3.3) to calculate the leaching rate.

306   Table 2 Cu and Pb contents in a sample

| Element	40% fly ash sample (g)	60% fly ash sample (g)
Cu	0.0309	0.0452
Pb	0.1006	0.1462

307
308   **4.2 Carbonation**

309   After being cured for 28 days, the cement-solidified fly ash samples were carbonated using the

310   CO_2 closed-cycle test system including the high-temperature and high-pressure reaction vessel,

311   as shown in Fig. 4 [21]. The closed-cycle system was designed to recycle the CO_2 and minimize

312   the amount of CO_2 entering the atmosphere. In the process of carbonation, the temperature was

313   primarily controlled by the chiller, and the pressure was controlled by the pump. The controlled

314   pressure and temperature curves are shown in Fig. 5. It is worth noting that the carbonation

315   simulations were run only for the duration when the pressure is stabilized.
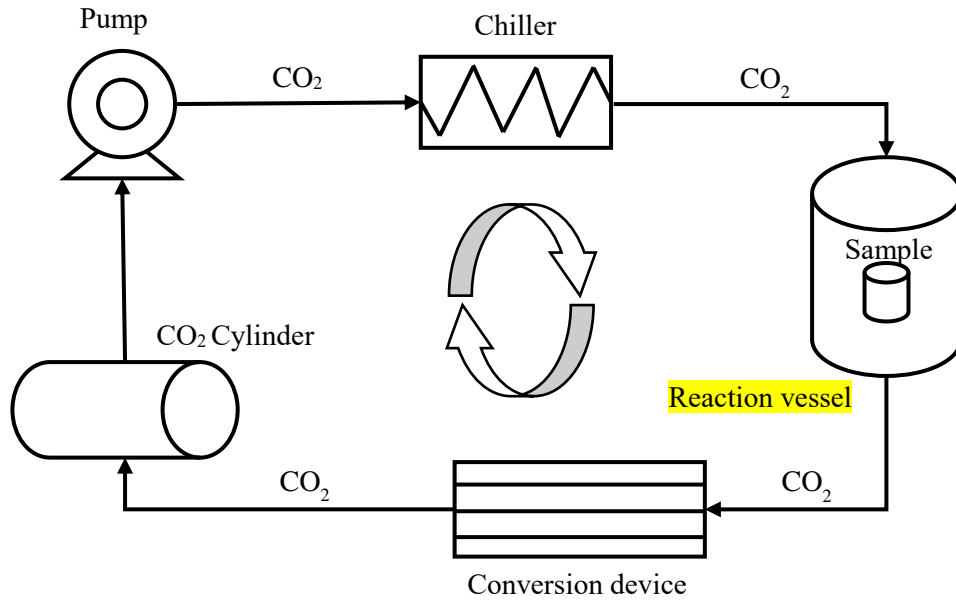
Fig. 4 CO_2 closed-cycle test system [21]
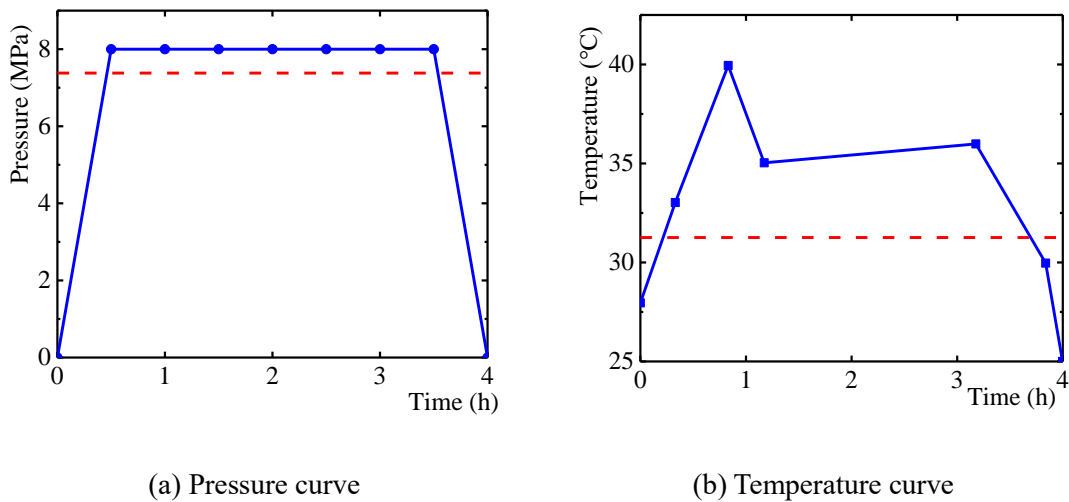

(a) Pressure curve

(b) Temperature curve

Fig. 5 Supercritical carbonation conditions

318
319 In order to determine whether the cement-solidified samples were carbonated, the mass of the

320 cement-solidified fly ash before and after carbonation were measured and is shown in Table 3.

321 The results show that the average percentages of mass increases of the samples are 5.416 (40%

322 fly ash) and 4.288 (60% fly ash), respectively. The mass increases of the samples with 40% fly

323 ash are generally larger than those of 60% fly ash, which is attributed to the larger amount of

324 mineral components (alkaline components) in the 40% than the 60% fly ash samples. The 40%

325 fly ash samples absorbed more CO_2, i.e. gained more weight than those of the 60% fly ash to

15

326 reach the same carbonation degree, which is also demonstrated by the calculation of c_{max} that

327 are 46.6 kg/m^3 and 34.1 kg/m^3, respectively for the 40% and 60% cement-solidified fly ash.

328 Table 3 Mass increase percentages of the cement-solidified samples after carbonation

Mass ratio of fly ash	Sample No	Mass before carbonation (g)	Mass after carbonation (g)	Mass increase percentage (%)	Average mass increase percentage (%)
40%	2/3-1	167.9	177.7	5.837	5.146
	2/3-4	170.6	179.7	5.334	
	2/3-6	172.5	180.5	4.638	
	2/3-10	173.3	181.8	4.905	
	2/3-11	164.5	171.7	4.377	
	2/3-14	164.5	174.0	5.775	
	2/3-16	169.5	176.4	4.071	
	2/3-19	168.5	176.4	4.071	
60%	3/2-6	164.0	170.8	4.146	4.288
	3/2-7	163.9	172.0	4.942	
	3/2-8	167.3	174.3	4.184	
	3/2-11	171.5	176.0	2.624	
	3/2-14	163.4	172.4	5.508	
	3/2-15	165.4	171.4	3.628	
	3/2-18	164.2	170.8	4.019	
	3/2-19	163.6	172.2	5.257	

329
330 In order to measure carbonation depth, the cross sections of the 40% and 60% fly ash samples

331 were, respectively, inspected. Phenolphthalein indicator was sprayed on the cut and the un-

332 carbonated zones changed color, as shown in Fig. 6. It is evident from the color change that

333 cement-solidified fly ash samples were carbonated as the CO_2 penetration from the outside

334 surfaces.
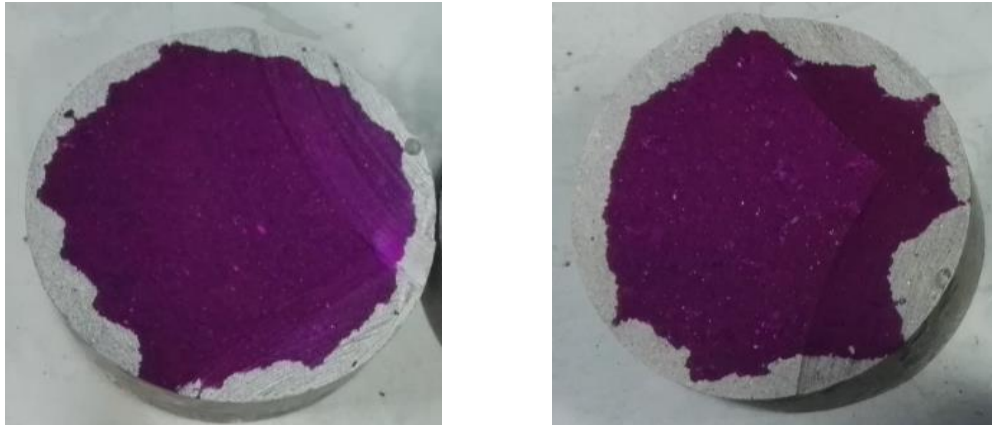
(a) 40% fly ash   (b) 60% fly ash

Fig. 6 Carbonation depth of the cement-solidified fly ash samples

335

336 Carbonation depths were measured at 88 points randomly selected along the carbonation front

337 of each samples. The average depths of the 40% and 60% fly ash sample are, respectively

338 2.1mm and 3.0mm. The test results agree well with the simulation carbonation depths based on

339 the modified model (respectively, 2.3mm and 3.5mm), but are significantly different with those

340 based on Zha et al. [27] (about 12mm). The results show that the capability of absorbing CO_2

341 varies with chemical compositions, which further influences carbonation depth. The above

342 comparisons confirm that using CO_2 absorption, c, rather than calcium carbonate production to

343 measure carbonation degree in simulations is more accurate.

344 **4.3 Strength test**

345 Strength tests were also carried out on the samples before and after carbonation. The cement-

346 solidified fly ash samples were divided into 4 groups in the test, i.e. the 40% cement-solidified

347 fly ash before and after carbonation; the 60% cement-solidified fly ash before and after

348 carbonation. Each un-carbonated group had 5 samples, while each carbonated group had 3

349 samples that had been carbonated for 3 hours under the supercritical condition. The test results

350 are listed in Table 4.

351   Table 4 Strength of the samples

Group	Sample No	Strength (MPa)	Average strength (MPa)
Non-carbonated 40% fly ash	2/3-12	23.4	20.9
	2/3-13	17.1	
	2/3-15	20.2	
	2/3-17	20.6	
	2/3-18	23.5	
Carbonated 40% fly ash	2/3-4	17.9	17.1
	2/3-6	16.7	
	2/3-14	16.7	
Non-carbonated 60% fly ash	3/2-3	9.1	9.1
	3/2-7	7.1	
	3/2-9	10.4	
	3/2-10	9.2	
	3/2-16	9.6	
Carbonated 60% fly ash	3/2-6	7.2	7.6
	3/2-11	7.8	
	3/2-19	7.8	

352

353 It is apparent from the test results that the overall strength of the carbonated samples is lower

354 than that of the samples before carbonation. This is different from Li [28] on cement blocks

355 without added fly ash, where the strength of cement block increased by more than 60% after

356 carbonation. For the cement blocks tested here, the replacement of cement by fly ash reduced

357 the size of pores [46], which made the block more sensitive to micro cracks due to the expansion

358 of pores caused by the calcium carbonate produced during carbonation process. The earlier

359 formation of the micro-cracks contributed to the reduction in strength of the cement-solidified

360 fly ash.

361
362 However, the results agree with Junior et al. [47], where the compressive strength of cement

363 paste decreased after being carbonated for 4 hours, though increase in strength occurred during

364 the first 1-2 hours carbonation. Junior et al. [47] also showed that the longer the carbonation

365 duration was (more than 4 hours), the greater the strength reduction would be. These might

366 attribute to the fact that the generated calcium carbonate had exceeded the limit of the pores,

which caused additional internal pressure and micro-crack [30]. In this paper, the cement-solidified fly ash was subject to supercritical carbonation, resulting to a quick accumulation of calcium carbonate in the pores and an earlier reduction in strength.

Table 4 also shows that the average strength of the 40% samples is more than twice that of the 60% samples for before and after carbonation, i.e., the strength of the cement-solidified samples is greatly reduced as the content of fly ash increases. The results agree with those of Lombardi et al. [48], which showed that the amount of strength reduction with fly ash/cement ratio varying from 0.75 to 1.5 was about 50% which is in line with the reduction (56.5% for un-carbonated samples, 55.6% for carbonated samples) observed from this study. In summary, the duration of carbonation and the proportion of fly ash added in cement-solidified fly ash should be properly administrated to optimize their recycling value.

4.4 Leaching experiment

4.4.1 Experiment equipment and process

The cement-solidified fly ash samples required simple surface treatment to remove stains before the leaching experiment. They were placed in pre-cleaned leaching containers. 1.2 L deionized water was injected into each of the containers to submerge the samples. The containers were then sealed and placed in a leaching chamber of constant temperature ready for the leaching experiment.

Twenty cement-solidified fly ash samples were tested in the leaching experiment, which were divided into 4 groups as shown in Table 5. Each of the groups have 5 samples with the same fly ash ratio and carbonation time. The total leaching time is 42 days. Leaching rates at days 1, 3, 7, 10, 14, 21, 28, 35 and 42 were measured and group averages were calculated.

Table 5 Details of leaching experiment

Group	Sample No	Leaching temperature(^oC)
Non-carbonated 40% fly ash	2/3-2,2/3-3,2/3-7,2/3-8,2/3-9	25

Group	Sample No	Leaching temperature(^oC)
Carbonated 40% fly ash	2/3-1,2/3-10,2/3-11,2/3-16,2/3-19	
Non-carbonated 60% fly ash	3/2-1,3/2-2,3/2-4,3/2-5,3/2-12	
Carbonated 40% fly ash	3/2-7,3/2-8,3/2-14,3/2-15,3/2-18	

393

394 The method recommended by GB/T 7023-2011 [43] was used to calculate the leaching rate of

395 the cement-solidified fly ash.

$$R_n = \frac{a_n / A_0}{(S/V)(\Delta t)_n} \tag{17}$$

396 where R_n is the leaching rate of heavy metals in the nth leaching period (cm/d), a_n is the leaching

397 mass in the nth leaching period (g), A_0 is the initial mass of heavy metals in the cement-solidified

398 fly ash (g), S is the contact area of the sample and leachant (cm^2), V is the volume of sample,
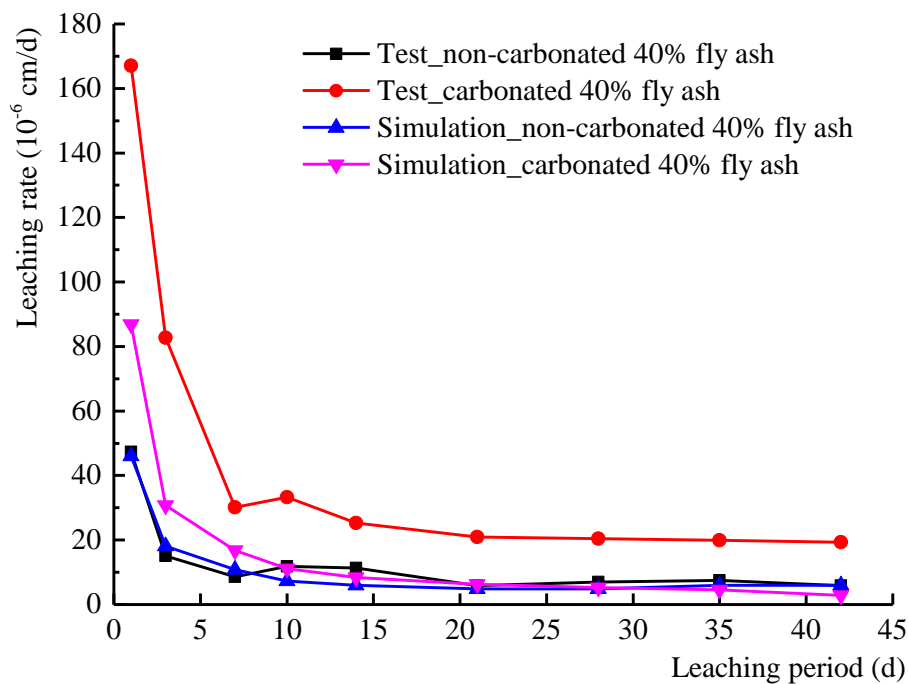
399 and $(\Delta t)_n$ is the days of the nth leaching period (d).

4.4.2 Results and analysis

401 The leaching rates of Cu in the 40% and the 60% cement-solidified fly ash are shown,

402 respectively, in Figs. 7 and 8, and those of Pb in the 40% and the 60% cement-solidified fly ash
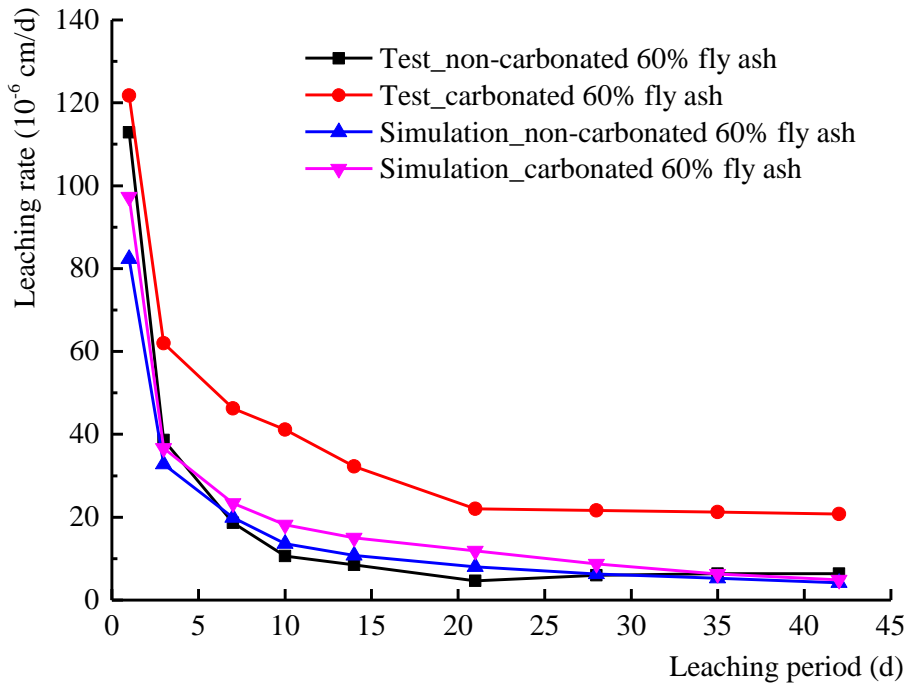
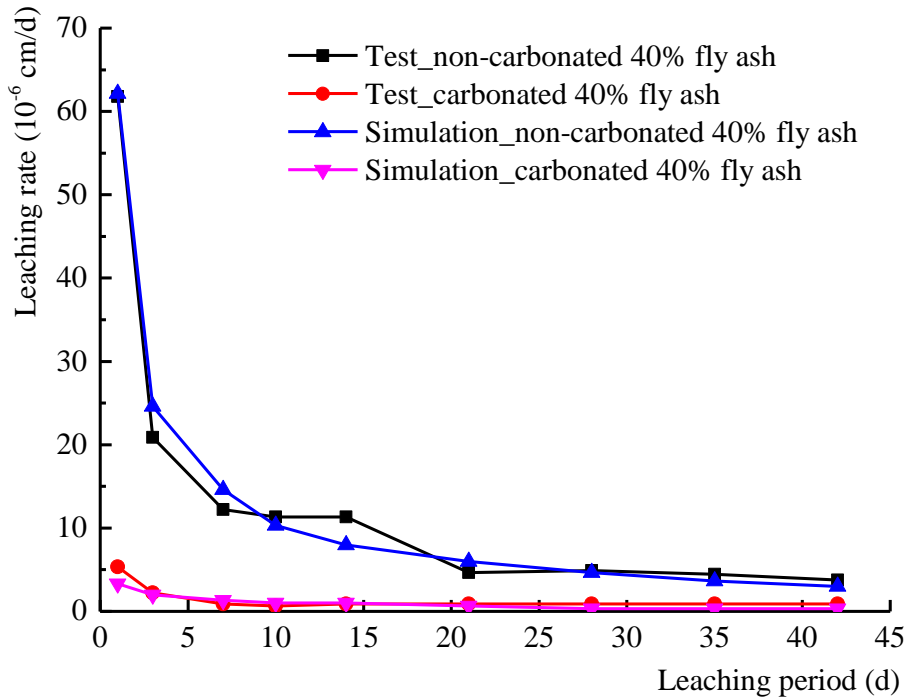403 are shown, respectively, in Figs. 9 and 10.

404

405 Fig. 7 Leaching rates of Cu in 40% cement-solidified fly ash

20

Fig. 8 Leaching rates of Cu in 60% cement-solidified fly ash
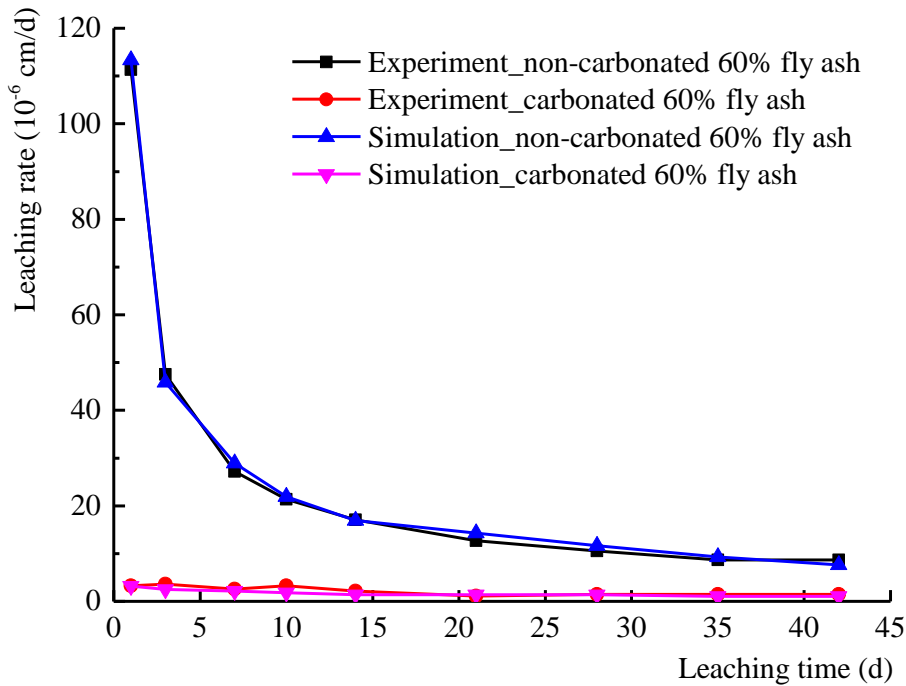
Fig. 9 Leaching rates of Pb in 40% cement-solidified fly ash

Fig. 10 Leaching rates of Pb in 60% cement-solidified fly ash

From Figs. 7-10, the simulated leaching rates of Pb agree well those measured in the leaching tests, while the agreement between the simulated and tested leaching rates of Cu are less satisfactory. This may be owing to that the calculation method of chemical activity factor for Cu (equation (15)) was not sufficiently accurate, which should include the impacts of not only the carbonation degree, but also the pH and ionic characteristics of the cement-based materials. Further research is required in this direction. Nevertheless, the modified model has correctly predicted the decrease of the leaching rate of Cu with increase of leaching time and the increase in leaching rate after the samples were carbonated (from the Figs. 7 and 8), which is consistent with the leaching tests results.

The leaching rate of Cu in carbonated cement-solidified fly ash is generally higher than that of the un-carbonated as shown in Figs. 7 and 8. The increased leaching of Cu from the cement-solidified samples is in line with the results of Valls and Vàzquez [49] and Ginneken et al. [25], but in contrast with the results of Gerven et al. [18], which may be due to the use of different types of fly ash, leachant pH, mixing ratio [19] and leaching procedures [48]. Based on the experiments of this paper, it is clear that carbonation does not help in retaining Cu in the cement-

based materials. One of the reasons is that carbonation leads to a decrease in pH of the cement-solidified fly ash (chemical retention), which deteriorates the chemical stability of Cu element in the form of hydroxide or carbonate under high-pH conditions, and is beneficial to the solubility of Cu element, thus increases the content of leachable Cu and its leaching rate [18]. The other is that though the calcium carbonate formed during the carbonation can block the leaching of the heavy metals (physical retention) [23, 50], the micro-crack induced by the over-carbonation can also promote leaching, and this may have occurred in this experiment. In addition, there is little difference in the long-term leaching rates of Cu in 40% and 60% cement-solidified fly ash, whether before or after carbonation. It can be seen from equation (17) that the leaching rate of leaching elements is proportional to the ratio of the leaching amount and the total amount of the leaching elements. In addition, for both Cu and Pb, Table 2 shows that the total amount of them is in proportional to the fly ash ratio. Thus, for a given leaching rate, the leaching amount of Cu varies linearly with fly ash ratio. A cement-solidified sample with higher fly ash ratio will leach more Cu.

The leaching rate of Pb of the carbonated cement-solidified fly ash was obviously lower than that of the un-carbonated (Figs. 9 and 10). The results agreed with those of Gerven et al. [18] and Sanchez et al. [51], but disagreed with those of Shafique et al. [52]. It is noteworthy to mention that the leaching in Shafique et al. [52] was mainly caused by micro-cracks after a significant decrease in porosity caused by carbonation. Because of the formation of lead carbonate ($PbCO_3$) from carbonation, Pb appears less solubility in neutral than high pH [18]. Hence, the leaching of Pb is influenced by both chemical and physical retentions. Considering the majority of the published results on leaching of Pb and the observations from this paper, it can be concluded that chemical retention has played a more important role than physical retention in reducing Pb leaching. Contrast to a rather constant long-term leaching rate of Cu for the samples with different fly ash ratios, the long-term leaching rate of Pb increases as the fly ash ratio increases. Hence, an increase of fly ash ratio will result in leaching more Pb than Cu, which can be accounted for that the amount of Pb is larger than that of Cu in fly ash (Table

2).

Overall, it can be concluded that the effect of carbonation on the leaching of heavy metals is not always favorable.

5. Conclusions

An existing supercritical carbonation model has been modified to consider carbonation of cement-solidified fly ash of various mixture ratios. This model was further combined with a leaching model to simulate leaching of heavy metals, i.e., Cu and Pb, in cement-solidified fly ash with and without being carbonated. Carbonation and leaching tests were carried out to verify the new models. The effect of supercritical carbonation on the properties of the cement-solidified fly ash were studied both numerically and experimentally. From the study the following observations have been made:

(1) Using CO_2 absorption instead of calcium carbonate to measure carbonation degree is more accurate in simulating carbonation process of cement-based materials with various mixtures.

(2) The strength of cement-solidified fly ash after carbonation may be reduced, depending on the carbonation duration and fly ash ratio.

(3) The leaching of Cu and Pb before and after carbonation have shown that carbonation is not always beneficial to the retention of heavy metals, depending on the combined effect of chemical and physical retentions.

(4) Leaching of Cu and Pb increases as fly ash ratio increases, while the increase in Pb leaching is more substantial.

Acknowledgements

492

493 **Reference**

494   [1]   C. Zhu, H. Tian, K. Cheng, K. Liu, K. Wang, S. Hua, J. Gao, J. Zhou, Potentials of whole

495   process control of heavy metals emissions from coal-fired power plants in China, J. Clean

496   Prod., 114 (2016) 343-351.

497   [2]   B. Prasad, K. Sangita, Heavy Metal Pollution Index of Ground Water of an Abandoned

498   Open Cast Mine Filled with Fly Ash: a Case Study, Mine Water Environ., 27 (2008) 265-

499   267.

500   [3]   S.A. Montzka, E.J. Dlugokencky, J.H. Butler, Non-CO2 greenhouse gases and climate

501   change, Nature, 476 (2011) 43-50.

502   [4]   J. Hays, Garbage and Recycling in China,

503   http://factsanddetails.com/china/cat10/sub66/item1111.html, 2014.

504   [5]   J. Tang, M. Petranikova, C. Ekberg, B.-M. Steenari, Mixer-settler system for the recovery

505   of copper and zinc from MSWI fly ash leachates: An evaluation of a hydrometallurgical

506   process, J. Clean Prod., 148 (2017) 595-605.

507   [6]   L. Wang, Q. Chen, I.A. Jamro, R.D. Li, H.A. Baloch, Accelerated co-precipitation of lead,

508   zinc and copper by carbon dioxide bubbling in alkaline municipal solid waste incinerator

509   (MSWI) fly ash wash water, RSC Adv., 6 (2016) 20173-20186.

510   [7]   J.B.M. Dassekpo, X.X. Zha, J.P. Zhan, J.Q. Ning, The effects of the sequential addition

511   of synthesis parameters on the performance of alkali activated fly ash mortar, Results in

512   Physics, 7 (2017) 1506-1512.

513   [8]   J.E. Aubert, B. Husson, N. Sarramone, Utilization of municipal solid waste incineration

514   (MSWI) fly ash in blended cement. Part 1: Processing and characterization of MSWI fly

515   ash, J. Hazard. Mater., 136 (2006) 624-631.

516   [9] L. Cang, Y.J. Wang, D.M. Zhou, Y.H. Dong, Heavy metals pollution in poultry and

517   livestock feeds and manures under intensive farming in Jiangsu Province, China, J.

518   Environ. Sci., 16 (2004) 371-374.

519   [10] E. Sakai, S. Miyahara, S. Ohsawa, S.H. Lee, M. Daimon, Hydration of fly ash cement,

520   Cement Concrete Res, 35 (2005) 1135-1140.

521   [11] L.H.J. Martin, F. Winnefeld, E. Tschopp, C.J. Muller, B. Lothenbach, Influence of fly ash

522   on the hydration of calcium sulfoaluminate cement, Cement Concrete Res, 95 (2017) 152-

523   163.

524   [12] J. Vargas, A. Halog, Effective carbon emission reductions from using upgraded fly ash in

525   the cement industry, J. Clean Prod., 103 (2015) 948-959.

526   [13] T. Hemalatha, A. Ramaswamy, A review on fly ash characteristics - Towards promoting

527   high volume utilization in developing sustainable concrete, J. Clean Prod., 147 (2017)

528   546-559.

529   [14] J.E. Aubert, B. Husson, A. Vaquier, Use of municipal solid waste incineration fly ash in

530   concrete, Cement Concrete Res, 34 (2004) 957-963.

531   [15] M. Arezoumandi, T.J. Looney, J.S. Volz, Effect of fly ash replacement level on the bond

532   strength of reinforcing steel in concrete beams, J. Clean Prod., 87 (2015) 745-751.

533   [16] M. Arezoumandi, J.S. Volz, Effect of fly ash replacement level on the shear strength of

534   high-volume fly ash concrete beams, J. Clean Prod., 59 (2013) 120-130.

535   [17] H.S. Shi, L.L. Kan, Leaching behavior of heavy metals from municipal solid wastes

536   incineration (MSWI) fly ash used in concrete, J. Hazard. Mater., 164 (2009) 750-754.

537   [18] T. Van Gerven, D. Van Baelen, V. Dutré, C. Vandecasteele, Influence of carbonation and

538   carbonation methods on leaching of metals from mortars, Cement Concrete Res, 34 (2004)

539   149-156.

540   [19] Q.J. Yu, S. Nagataki, J.M. Lin, T. Saeki, M. Hisada, The leachability of heavy metals in

541   hardened fly ash cement and cement-solidified fly ash, Cement Concrete Res, 35 (2005)

542   1056-1063.

543   [20] M. Moranville, S. Kamali, E. Guillon, Physicochemical equilibria of cement-based

544   materials in aggressive environments - experiment and modeling, Cement Concrete Res,

545   34 (2004) 1569-1578.

546   [21] X.X. Zha, H.Y. Wang, P.Y. Xie, C. Wang, P. Dangla, J.Q. Ye, Leaching resistance of

547   hazardous waste cement solidification after accelerated carbonation, Cem. Concr.

548   Compos., 72 (2016) 125-132.

549   [22] E.E. Berry, Fly Ash for Use in Concrete. Part 1, A Critical Review of the Chemical,

550   Physical and Pozzolanic Properties of Fly Ash, Energy, Mines and Resources Canada,

551   CANMET1976.

552   [23] A.V. Saetta, B.A. Schrefler, R.V. Vitaliani, The carbonation of concrete and the

553   mechanism of moisture, heat and carbon dioxide flow through porous materials, Cement

554   Concrete Res, 23 (1993) 761-772.

555   [24] P.J. Gunning, C.D. Hills, P.J. Carey, Accelerated carbonation treatment of industrial

556   wastes, Waste Management, 30 (2010) 1081-1090.

557   [25] L. Van Ginneken, V. Dutre, W. Adriansens, H. Weyten, Effect of liquid and supercritical

558   carbon dioxide treatments on the leaching performance of a cement-stabilised waste form,

559   Journal of Supercritical Fluids, 30 (2004) 175-188.

560   [26] J.Y. Shen, P. Dangla, M. Thiery, Reactive transport modeling of CO2 through

561   cementitious materials under CO2 geological storage conditions, Int. J. Greenh. Gas

562   Control, 18 (2013) 75-87.

563   [27] X.X. Zha, M. Yu, J.Q. Ye, G.L. Feng, Numerical modeling of supercritical carbonation

564   process in cement-based materials, Cement Concrete Res, 72 (2015) 10-20.

565   [28] Y. Li, The theoretical and experimental study of supercritical carbon dioxide on

566   transforming cement-base building materials, Harbin Institute of Technology, 2012.

567   [29] G. Feng, Experimental and numerical study of accelerated carbonation in cement brick

568   and tile, Harbin Institute of Technology, 2013.

569   [30] M.G. Richardson, Carbonation of reinforced concrete: its causes and management,

570   University College Dublin, 1988.

571   [31] V.G. Papadakis, C.G. Vayenas, M.N. Fardis, Fundamental modeling and experimental

572   investigation of concrete carbonation, ACI Mater. J., 88 (1991) 363-373.

573   [32] Chemical reagent-Preparations of reagent solutions for use in test methods, GB/T 603-

574   2002.

575   [33] L. Chen, Research on concrete carbonation model and its parameters, Xi'an University of

576   Architecture and Technology, 2007.

577   [34] J.-B.M. Dassekpo, X. Zha, J. Zhan, J. Ning, The effects of the sequential addition of

578   synthesis parameters on the performance of alkali activated fly ash mortar, Results in

579   Physics, 7 (2017) 1506-1512.

580   [35] J.B.M. Dassekpo, J.Q. Ning, X.X. Zha, Potential solidification/stabilization of clay-waste

581   using green geopolymer remediation technologies, Process Saf. Environ. Protect., 117

582   (2018) 684-693.

583   [36] I. Phummiphan, S. Horpibulsuk, R. Rachan, A. Arulrajah, S.-L. Shen, P. Chindaprasirt,

584   High calcium fly ash geopolymer stabilized lateritic soil and granulated blast furnace slag

585   blends as a pavement base material, J. Hazard. Mater., 341 (2018) 257-267.

586   [37] W. Jie, J.B.M. Dassekpo, C.Y. Wan, X.X. Zha, Experimental and numerical modeling of

587   chloride diffusivity in hardened cement concrete considering the aggregate shapes and

588   exposure-duration effects, Results in Physics, 7 (2017) 1427-1432.

589   [38] J. Li, X. Zhao, Z. Liu, A new equation for calculating specific heat capacity of

590   supercritical fluid, Proceedings of the 2009 Conference on Engineering

591   Thermodynamics and Energy UtilizationDalian, 2009, pp. 1-6.

592   [39] L. Shi, X.F. Zhang, X.G. Zhang, B.X. Han, G.Y. Yang, H.K. Yan, Constant-Volume Heat

593   Capacity of Mixed Supercritical Fluids and Molecular Interaction in the Systems, Chinese

594   Chemical Letters, (1999) 873-874.

595   [40] S.J. Kwon, H.W. Song, Analysis of carbonation behavior in concrete using neural network

596   algorithm and carbonation modeling, Cement Concrete Res, 40 (2010) 119-127.

597   [41] N.R. Short, P. Purnell, C.L. Page, Preliminary investigations into the supercritical

598   carbonation of cement pastes, Journal of Materials Science, 36 (2001) 35-41.

599 [42] Y. Song, Y. Wang, P. Song, Q. Li, Nonequilibrium Thermodynamics Study of Nuclide

600　　 Migration Behavior in the Cement Based Radioactive Waste Forms, Journal of Henan

601　　 University(Natural Science), (2006) 21-24.

602 [43] Standard test method for leachability of low and intermediate level solidified radioactive

603　　 waste forms, GB/T 7023-2011.

604 [44] F.R. Wu, Y. Masuda, S. Nakamura, S. Sato, Influence of mixture proportion and curing

605　　 condition on contribution of fly ash to strength of concrete, in: N.Q. Feng, G.F. Peng (Eds.)

606　　 Environmental Ecology and Technology of Concrete, Trans Tech Publications Ltd,

607　　 Zurich-Uetikon, 2006, pp. 235-241.

608 [45] E. L. White, D. M. Roy, P. D. Cady, Modeling the Effects of Fly Ash Characteristics and

609　　 Mixture Proportions on Strength and Durability of Concretes, 1986.

610 [46] P. Chindaprasirt, C. Jaturapitakkul, T. Sinsiri, Effect of fly ash fineness on compressive

611　　 strength and pore size of blended cement paste, Cem. Concr. Compos., 27 (2005) 425-

612　　 428.

613 [47] A. Neves Junior, R.D. Toledo Filho, E.d.M. Rego Fairbairn, J. Dweck, A study of the

614　　 carbonation profile of cement pastes by thermogravimetry and its effect on the

615　　 compressive strength, Journal of Thermal Analysis and Calorimetry, 116 (2014) 69-76.

616 [48] F. Lombardi, T. Mangialardi, L. Piga, P. Sirini, Mechanical and leaching properties of

617　　 cement solidified hospital solid waste incinerator fly ash, Waste Management, 18 (1998)

618　　 99-106.

619 [49] S. Valls, E. Vàzquez, Accelerated carbonatation of sewage sludge‐cement–sand mortars

620　　 and its environmental impact, Cement Concrete Res, 31 (2001) 1271-1276.

621 [50] P.J. Dewaele, E.J. Reardon, R. Dayal, Permeability and porosity changes associated with

622　　 cement grout carbonation, Cement Concrete Res, 21 (1991) 441-454.

623 [51] F. Sanchez, C. Gervais, A.C. Garrabrants, R. Barna, D.S. Kosson, Leaching of inorganic

624　　 contaminants from cement-based waste materials as a result of carbonation during

625　　 intermittent wetting, Waste Management, 22 (2002) 249-260.

626   [52] M.S.B. Shafique, J.C. Walton, N. Gutierrez, R.W. Smith, A.J. Tarquin, Influence of

627   carbonation on leaching of cementitious wasteforms, J. Environ. Eng.-ASCE, 124 (1998)

628   463-467.

629